Biomimetic Presentation of Cryptic Ligands via Single-Chain Nanogels for Synergistic Regulation of Stem Cells

DOI:
10.1021/acsnano.9b08564

Document Version
Accepted author manuscript

Biomimetic Presentation of Cryptic Ligands via Single-Chain Nanogels for Synergistic Regulation of Stem Cells

Journal:	*ACS Nano*
Manuscript ID	nn-2019-08564u.R5
Manuscript Type:	Article
Date Submitted by the Author:	27-Mar-2020
Complete List of Authors:	Chen, Xiaoyu; Chinese University of Hong Kong, Mechanical and Automation Engineering Lai, Nathanael Chun-Him; Chinese University of Hong Kong Wei, Kongchang; Empa, Swiss Federal Laboratories for Materials Science and Technology, Laboratory for Biomimetic Membranes and Textiles Li, Rui; Chinese University of Hong Kong Cui, Miao; City University of Hong Kong Yang, Boguang; Chinese University of Hong Kong Wong, Siu Hong Dexter; The Chinese University of Hong Kong, Biomedical Engineering Deng, Yingrui; Chinese University of Hong Kong Li, Jiashen; University of Manchester, Department of Materials Shuai, Xintao; Sun Yat-Sen University, School of Materials Science and Engineering Bian, Liming; the Chinese University of Hong Kong, Biomedical Engineering

Biomimetic Presentation of Cryptic Ligands *via* Single-Chain Nanogels for Synergistic Regulation of Stem Cells

Xiaoyu Chen,[†,‡] Nathanael Chun-Him Lai,[†,‡] Kongchang Wei,[⊥,‡] Rui Li,[†] Miao Cui,[‖] Boguang Yang,[†] Siu Hong Dexter Wong,[†] Yingrui Deng,[†] Jiashen Li,[Ψ] Xintao Shuai,[Ø] and Liming Bian*[, †, ¶]

[†] Department of Biomedical Engineering, The Chinese University of Hong Kong, Hong Kong SAR, 999077, P. R. China

[⊥] Empa, Swiss Federal Laboratories for Materials Science and Technology, Laboratory for Biomimetic Membranes and Textiles, Lerchenfeldstrasse 5, CH-9014 St. Gallen, Switzerland.

[‖] Department of Biomedical Sciences, City University of Hong Kong, Hong Kong SAR, 999077, P. R. China

[Ψ] Department of Materials, The University of Manchester, Manchester, M13 9PL, U. K.

[Ø] PCFM Lab of Ministry of Education, School of Materials Science and Engineering, Sun Yat-sen University, Guangzhou 510275, P. R. China.

[¶] Shenzhen Research Institute, The Chinese University of Hong Kong, Sha Tin, New Territories 999077, Hong Kong, P. R. China.

Corresponding Author: * lbian@cuhk.edu.hk.

ABSTRACT: Dynamic controlling the nanoscale presentation of synergistic ligands to stem cells by biomimetic single-chain materials can provide critical insights to understand the molecular crosstalk underlying cells and their extracellular matrix. Here, a stimuli-responsive single-chain macromolecular nano-regulator with conformational dynamics is fabricated based on advanced scale-up single polymeric chain nanogel (SCNG). Such carefully-designed SCNG is capable of mediating triggered co-presentation of the master and cryptic ligands in a single molecule to elicit the synergistic crosstalk between different intracellular signaling pathways, thereby considerably boosting the bioactivity of the presented ligands. This controllable nanoswitching-on of cell-adhesive ligands' presentation allows regulation of cell adhesion and fate from molecular scale. The modular nature of this synthetic macromolecular nano-regulator makes it a versatile nanomaterial platform to assist basic and fundamental studies in a wide array of research topics.

KEYWORDS: single-chain nanogel • stem cells regulation • cryptic ligands presentation • stimuli-responsive nano-regulator • synergistic ligands

Many studies have demonstrated that cell behaviors can be regulated by the interaction between the receptors on the cell surface and the ligand motifs present in the extracellular matrix (ECM) components.[1, 2] Such ligand-receptor ligation is an indispensable triggering event initiating the majority of intracellular signaling cascades.[3-6] One of the most well-known ligands for regulating cell adhesion to ECM is the Arg-Gly-Asp (RGD) peptide sequence which can be found in many ECM components such as fibronectin and collagen. The cell adhesion behaviors can be regulated by the dynamic binding of RGD peptide ligands to the cell surface receptors, such as integrins. The recognition and binding of integrins to the adhesive ligands initiate formation of the cell adhesion structures which mediate cellular forces and mechanotransduction signaling. The resultant cell traction force is highly dynamic and depends on the binding kinetics of integrins to the peptide ligands.[7] In addition, our recent study showed that the presentation of a Wnt5a mimetic peptide, Foxy5 peptide (formyl-Met-Asp-Gly-Cys-Glu-Leu),[8-10] can enhance the mechanosensing-dependent osteogenesis of human mesenchymal stem cells (hMSCs) through the activation of noncanonical Wnt signaling.[11-14] Noncanonical Wnt signaling is known to play an essential role in regulating the mechanotransduction and focal adhesion formation of cells by regulating the actomyosin assembly.[15-20]

In addition to supplying a single functional peptide, simultaneous presentation of multiple ligands in close physical proximity to cells can generate potential crosstalks among the different activated signaling pathways, thereby further potentiating and complicating the downstream signaling events.[1, 6, 21, 22] In the natural cell microenvironment, many biomacromolecules can present multiple ligands in a single molecule and synergize their effect on regulating cellular functions.[2, 23] For example, fibronectin can bind to integrin receptors *via* its cell-adhesive domain and simultaneously mediate binding of sequestered growth factors to their receptors, and the

proximity of these dual ligations substantially enhances growth factor signaling.[24] Furthermore, the conformational changes in these biomacromolecules in response to environmental stimuli, such as protein unfolding due to cellular forces, can expose cryptic receptor-binding sites, and such dynamic presentations of hidden ligands enable the spatiotemporal regulation of the ligand-receptor ligations and associated signaling events.[25]

To mimic the complex structures and functions of natural macromolecules, synthetic macromolecule-based nanomaterials with stimuli-responsive dynamic presentation of multiple bioactive ligands in a single polymer chain can provide valuable insight and foster the development of the effective therapies for regenerative medicine, cancer immunotherapy, and major infectious diseases.[7, 26-28] Single polymeric chain nanogel (SCNG) can significantly enhance the stability and efficiency of the functional biomolecules, and the protein-encapsulating nanogels are highly desirable for protein therapy.[29] Previous studies have proposed several delicate strategies for direct encapsulation of proteins by responsive polymeric nanocapsules *via in-situ* polymerization method.[30, 31] Compared to the previous methods, in this study, we developed a different bottom-up method to prepare the bio-functional single polymeric chain-based nanogels which can accommodate easy conjugation of multiple bioactive ligands.[21] Furthermore, our strategy allows the preparation of customized SCNGs with varying chemical structures and different stimuli-responsiveness by using different monomers and intra-chain crosslinkers. In this work, we evaluate the efficacy of such polymeric SCNGs in mediating the controlled dynamic nanoscale presentation of dual bioactive ligands in a single synthetic molecule. Based on this SCNG-based dynamic regulator, we further investigate the potential synergistic action on stem cells by the proximal co-presentation of two model ligands, *i.e.*, RGD peptide, a widely used integrin-binding peptide, and

the Foxy5 peptide,[8-10] a Wnt5a biomimetic peptide capable of initiating noncanonical Wnt signaling upon ligation to its receptor.[11-14, 32-34]

RESULTS AND DISCUSSION

Preparation of reduction-responsive SCNGs containing cryptic cell adhesive ligands

We synthesized a biomimetic nano-regulator for co-presentation of synergistic ligands based on single-chain nanogels (SCNGs) by using our recently developed scale-up method.[21] In brief, we used the *S, S'*-bis(α'α'-dimethyl-α''-propargyl acetate) *tri*thiocarbonate (BDPT, **Figure S1**) as the symmetrical chain transfer agent (CTA) for mediating the reversible addition-fragmentation chain transfer (RAFT) polymerization of *N, N*-dimethyl acrylamide (DMA) to produce an ABA-type block copolymer. *N, N'*-cystaminebisacrylamide (CBA, containing disulfide bonds) was copolymerized in the central B domain to introduce reduction-cleavable intrachain crosslinks, which induce the folding of the central B domain, thereby concealing the copolymerized RGD peptide in the folded B domain (**Figure 1a**). The obtained CBA-SCNG-RGD can be unfolded to expose the concealed RGD peptide under reducing conditions upon cleavage of disulfide bonds in the CBA cross-linker. The number of RGD peptides embedded in each SCNG can be determined from the ^{1}H NMR characterization (**Figure S2**), and the result is consistent with the feeding ratio used for the synthesis of SCNGs (Supporting Information, **Table S1**).

The obtained CBA-SCNG-RGD has a narrow and unimodal molecular weight distribution with relative low polydispersity index (PDI) values (1.22-1.32) as determined by gel permeation chromatography (GPC, **Figure S3a, Table S1**), indicating the successful preparation of SCNG

without multi-chain species.[35-37] In addition, the GPC data also reveals the reduction-induced unfolding behavior of the SCNGs by showing a change in elution time (obtained by GPC-RI) but no change in the absolute weight-averaged molecular weight (obtained by GPC-MALS) upon adding the tris(2-carboxyethyl)phosphine (TCEP) as the reducing agent **(Figure S3a)**. Dynamic light scattering (DLS) analysis also revealed a slight decrease in the hydrodynamic radius (R_H) of the SCNGs from 6.3 nm to 4.8 nm upon TCEP-induced unfolding (**Figure S3b**). The decrease in size of the SCNGs upon unfolding is likely due to the transformation of the extended wing blocks of folded SCNGs to the floppy and contracted conformation upon unfolding of the central domain (**Figure S4**), which was also shown in previous studies.[37-39]

The successful preparation of SCNGs is also confirmed by atomic force microscopy (AFM, **Figure 1c**). SCNGs deposited on silica wafers show an average height of approximately 7-11 nm. Furthermore, the small-angle X-ray scattering (SAXS) analysis of the macro-CTA (A block) is featureless (**Figure 1d, Table S2**) and fits well with the generalized Gaussian chain model by the SAXSgui software.[40, 41] In contrast, the scattering curve of the CBA-SCNG-RGD (**Figure 1d**) clearly shows an additional feature at approximately q = 0.7 nm^{-1} and fits well with a combined sphere and Gaussian chain model (**Figure 1e**). This scattering feature indicates the existence of central domains with higher mass density than that of their surrounding environments, thereby confirming the successful preparation of folded SCNGs. Upon unfolding of the SCNGs, the scattering curve of the unfolded SCNGs becomes featureless and fits well to the Gaussian chain model again (**Figure 1f**), indicating the unfolding of the SCNGs upon reduction, and this is in accordance with the GPC and DLS observation (**Figure S3**). We also prepared non-unfoldable SCNGs as control groups by utilizing *N, N′*-methylenebisacrylamide (MBA) as the uncleavable cross-linker (MBA-SCNG-RGD) (**Figure S5**). MTT assay results showed minimal cytotoxicity of

CBA-SCNG-RGD and MBA-SCNG-RGD, indicating the excellent cytocompatibility of SCNGs (**Figure S6)**.

Additional conjugation of Wnt5a mimetic peptide as the second ligand in the SCNGs

With the RGD ligand concealed inside the folding domain of SCNGs, we further conjugated the Wnt5a mimetic peptide ligand, Foxy5, to one of the functional alkynyl groups on the SCNGs. SCNGs as a tunable linker of these two ligands were immobilized onto thiolated glass substrates (**Figure 1b**). The modification of Foxy5 peptide onto SCNGs was based on the efficient "thiol-yne" click reaction. According to the thiol-yne reaction mechanism, each yne group will first react with a single thiol moiety to form a vinyl-sulfide structure. Subsequently, such a vinyl-sulfide structure will react with another thiol moiety, yielding the disubstituted adduct. The reaction between vinyl-sulfide and thiol has much faster reaction kinetics than the first step reaction between the yne moiety and thiol group.[24, 25] Therefore, there should be two Foxy5 peptides reacted with each SCNG immobilized on the glass. The number of conjugated Foxy5 peptides in each SCNG was also confirmed by ^{1}H NMR (**Figure S2**). The conjugated Foxy5 ligand can activate the noncanonical Wnt signal pathway and promote the osteogenic differentiation of hMSCs, while the concealed RGD ligand is designed to be exposed to the cells in response to a reduction trigger, whereafter promoting cell mechanosensing and differentiation synergistically. We utilized the scanning electron microscopy (SEM) to further confirm the modification of SCNGs on glass substrates. After washing with water for five times, the SCNG-modified substrates were dried for 24 hours before being mounted on copper studs and sputter-coated with gold for 1 min for SEM imagining. The obtained images show that the immobilized SCNGs have an average diameter of 10 ± 2.5 nm, and the substract has an average particle density of 42 ± 11 particles/μm^2 in its dehydrated state (**Figure S7**).

Triggered presentation of cryptic ligands from SCNGs enhances mechanosensing of stem cells

To examine the putative synergistic effect of RGD and the Foxy5 peptide, we further conjugated MBA-SCNG-RGD-Foxy5 (non-unfoldable), CBA-SCNG-RGD (unfoldable but without Foxy5), and MBA-SCNG-RGD (non-unfoldable and without Foxy5) onto the substrate as controls. After the coating with the SCNGs, the substrate was treated by bovine serum albumin (BSA) to avoid the nonspecific cellular adhesion. The cells were seeded onto the SCNG-immobilized substrates for 4 hours to ensure the cell-substrate adhesion. Then 10 μM TCEP was added into the culture medium to induce the unfolding of SCNGs. After 30 min, the reduction agent was removed by replacing the culture medium. The treated groups were further incubated for 12 hours before they were washed with DPBS and fixed with 4% w/v paraformaldehyde at pH 7.2-7.4 for 15 min at 25 ºC. Only a few attached cells were found on substrates with non-unfoldable MBA-SCNG-RGD or MBA-SCNG-RGD-Foxy5 linkers, and the adherent cells developed spindle-like morphology with a small spreading area (**Figure 2a, 2b**). This result indicates that MBA-SCNG can effectively hide the RGD ligand and hamper cell adhesion as well as spreading. On the contrary, the number of adherent cells and the size of the cell spreading area in the CBA-SCNG-RGD and CBA-SCNG-RGD-Foxy5 groups are significantly higher than that of MBA-SCNGs-RGD and MBA-SCNG-RGD-Foxy5 groups because of the increased RGD presentation in the unfoldable CBA-SCNGs groups (**Figure 2a, 2b**). Furthermore, hMSCs in the CBA-SCNG-RGD-Foxy5 group developed more punctate vinculin accumulation and pronounced actin stress fibers, which could give rise to better mechanotransduction for cell adhesion, as revealed by immunostaining (**Figure 2b**). However, hMSCs cultured on substrates with concealed RGDs (MBA-SCNGs-RGD and MBA-SCNG-RGD-Foxy5) developed significantly less punctate

vinculin and filamentous actin (**Figure 2b**). These results prove that the reduction-induced unfolding of the CBA-SCNG linker can efficiently increase the presentation of the concealed RGD and promote cell adhesion and mechanosensing. Furthermore, hMSCs cultured on the CBA-SCNG-Foxy5 substrates also exhibited significantly more nuclear localization of the key mechanosensing transcription factor, yes-associated protein (YAP), than that of substrates with only presented RGD (CBA-SCNG) or Foxy5 (MBA-SCNG-Foxy5) (**Figure 2b-c**). This finding suggests that the co-presentation of Foxy5 and RGD ligand achieved by the unfolding of CBA-SCNGs synergistically promotes the mechanotransduction signaling of hMSCs on CBA-SCNG-RGD-Foxy5 substrates.

Co-presentation of the dual ligands by SCNGs synergistically enhances the differentiation of stem cells

We next investigated the impact of SCNG-based ligand co-presentation on osteogenic differentiation of hMSCs. after 7 days of culture on the aforementioned substrates in osteogenic induction medium. The cells were first seeded onto the aforementioned different groups of substrates and incubated for 4 hours to ensure cell adhesion. TCEP was then added to the medium to induce the unfolding of SCNGs. After 30 min, the cell-laden substrats were further washed with osteogenic induction medium before being subjected to culturing for 7 more days. Consistent with the observation at 12 hours, cells on the CBA-SCNG-RGD and CBA-SCNG-RGD-Foxy5 groups spreaded more and developed more prominent focal adhesions (FAs) (**Figure 3a**) than the cells on the MBA-SCNG-RGD-Foxy5 substrate. The MBA-SCNG-RGD group showed the least cell adhesion and spreading. The immunofluorescence staining for Runt-related transcription factor 2 (RUNX2), a key transcription factor associated with osteogenic differentiation, also indicated that the co-presentation of dual ligands leads to a high level of RUNX2 nuclear localization in cells.

The nuclear RUNX2 fluorescence intensity in the CBA-SCNG-RGD-Foxy5 group was 172%, 227%, and 193% higher than that in the CBA-SCNG-RGD, MBA-SCNG-RGD, and MBA-SCNG-RGD-Foxy5 groups, respectively (**Figure 3b**). To further comfirm the efficacy of utilizing SCNGs to regulate cell fate, we stained the hMSCs against alkaline phosphatase (ALP), a maker enzyme produced in mature osteogenic cells, after culturing for 7 days in osteogenic induction medium. The ALP staining results showed that the CBA-SCNG-RGD-Foxy5 group had the highest ALP activity (**Figure 3a**).

To verify the synergy of co-presentation of dual ligands in the same SCNG, we conjugated CBA-SCNG-RGD (providing RGD only) and CBA-SCNG-Foxy5 (providing Foxy5 only) in an equal molar mixture on the substrate (denoted as MIX-RGD-Foxy5), and the total number of RGD and Foxy5 peptide used in the control group was kept the same as that of the CBA-SCNG-RGD-Foxy5 group. After 7 days of culture, the ALP staining intensity of the MIX-RGD-Foxy5 group was obviously weaker than that of the CBA-SCNG-RGD-Foxy5 group. To quantify the osteogenic differentiation level of hMSCs in each group, we used real-time polymerase chain reaction (qPCR) to analyze the expression of main osteogenic marker genes. Consistent with the ALP staining results, the RT-PCR data show that cells cultured on the CBA-SCNG-RGD-Foxy5 surface had significantly up-regulated expression of osteogenic marker genes, including ALP, RUNX2, osteocalcin (OCN), and type I collagen (Col I), compared with that of all other groups. Alizarin red staining also indicated that the cells on the CBA-SCNG-RGD-Foxy5 substrate have more calcification than that of all the other control groups (**Figure 3b**). This result indicates that the co-presentation of RGD and Foxy5 peptides on the same SCNG (CBA-SCNG-RGD-Foxy5 group) may represent a more optimized co-presentation of these two ligands than the separate presentation of these two ligands in different SCNGs.

Although very few studies have reported the interaction and synergy between integrin and Wnt5a receptor, a previous study showed that the proximity presentation of a cell-adhesive ligand with a growth factor could synergistically boost the bioactivity of growth factor.[22] In this work, the co-presentation of RGD and Foxy5 peptide on the same SCNG may promote the physical proximity of the specific receptors of these two ligands, thereby synergistically activating the non-canonical Wnt signaling by Foxy5 peptide together with the adjacent RGD-integrin binding. Such simultaneous activation of non-canonical Wnt signaling and integrin-based signaling *via* proximity presentation of the two different ligands may have contributed to the enhanced formation of focal adhesion, mechanotransduction signaling, and stem cell differentiation. These findings suggest that the co-presentation of RGD and Foxy5 by dynamic SCNGs can activate both integrin-mediated mechanotransduction and noncanonical Wnt and synergistically promote the osteogenic differentiation of stem cells (**Figure 3c**). Moreover, only the co-presentation of dual ligands on the same SCNG but not on separate SCNGs can synergistically promote stem cell differentiation.

CONCLUSIONS

In summary, we develop a conformationally dynamic single-chain nanogel as a stimuli-responsive single-chain macromolecular nano-regulator to mediate synergistic ligand presentation and elicit crosstalk between different intracellular signaling pathways. Ligand-receptor binding is the driving molecular mechanism underlying numerous cellular behaviors and functions. Our biomimetic SCNG-based macromolecular regulator can be greatly instrumental to the investigation of the impact of nanoscale ligand presentations on the behaviors and functions of various cell types, including stem cells, cancer cells, and immune cells.

METHODS

Preparation of the macro-CTA

For the preparation of macro-CTA-100, macro-CTA-200, macro-CTA-300, and macro-CTA-500, dimethylacetamide (DMA, 1.98 g; 3.96 g; 5.94g; 9.75 g), azobisisobutyronitrile (AIBN, 3.2 mg,) and *S, S'*-bis(α'α'-dimethyl-α''-propargyl acetate) *tri*thiocarbonate (BDPT, 56.4 mg) were dissolved in 10 mL, 20 mL, 30 mL, and, 50 mL dioxane respectively. After bubbling nitrogen for 15 min, the sealed bottle was then immersed in a 70 °C oil bath for two hours. Then the polymerization was quenched by cooling down the reaction with liquid nitrogen. Then the reaction mixture was added into 10 times of diethyl ether (by volume) dropwise to get the macro-CTA as precipitates. The crude products were collected by centrifugation at 5000 r.p.m. , and further washed by diethyl ether for two more times, and dried by vacuum.

Preparation of CBA-SCNGs and MBA-SCNGs with concealed RGD ligands

The prepared PDMAm was used as the macro-CTA to mediate the RAFT polymerization. *N, N*-Dimethylacrylamide (DMA), *N, N'*-methylenebis(acrylamide) (MBA) or *N, N'*-cystaminebisacrylamide (CBA) (cross-linker), acrylate RGD, and AIBN were dissolved in dioxane at a specific concentration. After bubbling nitrogen for 15 min, the sealed bottle was then immersed in a 70 °C oil bath for two hours. Then the polymerization was quenched by cooling down the reaction with liquid nitrogen. Then the reaction mixture was added into 10 times of diethyl ether (by volume) dropwise to get the SCNGs as precipitates. The crude product was collected by centrifugation at 5000 r.p.m. , and further washed by diethyl ether for two more times, and dried under vacuum. The obtained SCNGs were denoted as CBA_x-$SCNG_m^n$-RGD_y and MBA_x-$SCNG_m^n$-RGD_y, with n, x, and y representing the feeding molar ratio between the second block monomer

DMA (n), crosslinker (x) and RGD ligand (y); with m representing the number of repeating units from macro-CTA used to mediate the polymerization. No macroscopic precipitation was observed during the polymerization, and the GPC-RI and GPC-MALS was used to characterize the yielded SCNGs.

Preparation of substrates conjugated with CBA-SCNG-RGD-Foxy5 and MBA-SCNG-RGD-Foxy5.

The Foxy5 peptide was conjugated to the prepared CBA-SCNG-RGD or MBA-SCNG-RGD by the thiol-alkynyl reaction. Specifically, 50 mg of CBA-SCNG-RGD (Mw = 30000) and 2.2 mg of Foxy5 was dissolved in 1.5 mL DMSO with 0.01% I2959 as the UV initiator. The mixture solution was exposed to UV irradiation for 30 min. Then the above solution was transferred onto the thiolated substrate, followed by another 30 min UV exposure for immobilizing the SCNGs onto the substrates. The substrates were then immersed in 5% w/v BSA/PBS solution for 1 hour before cell culture experiments.

Cell Culture and treatments

All cell culture experiments throughout this study were conducted at 37 ºC with 5% CO_2. hMSCs (passage 5) were seeded at a constant density of 10,000 cells/cm^2 onto the CBA-SCNG-RGD, MBA-SCNG-RGD, CBA-SCNG-RGD-Foxy5, and MBA-SCNG-RGD-Foxy5 modified substrates (10 mm Ø, Marienfeld) in a 24-well culture plate under basal medium, *i.e.*, alpha-Minimum Essential Medium supplemented with 10% FBS, 1% streptomycin /penicillin, and 1% L-glutamine. The cells were cultured on the SCNG substrates for 4 hours to ensure proper adhesion before the addition of 10 μM TCEP in cell culture medium. After 30 min, TCEP was removed by washing with culture medium twice. The cells were incubated for 12 hours and then fixed. For

evaluation of cell differentiation effect, hMSCs were cultured in osteogenic induction medium (*i.e.*, basal medium added with 10 mM BPG, 50 μg/mL L-ascorbic acid 2-phosphate, and 100 nM dexamethasone) for 7 days after 1 day of cell adhesion in basal medium.

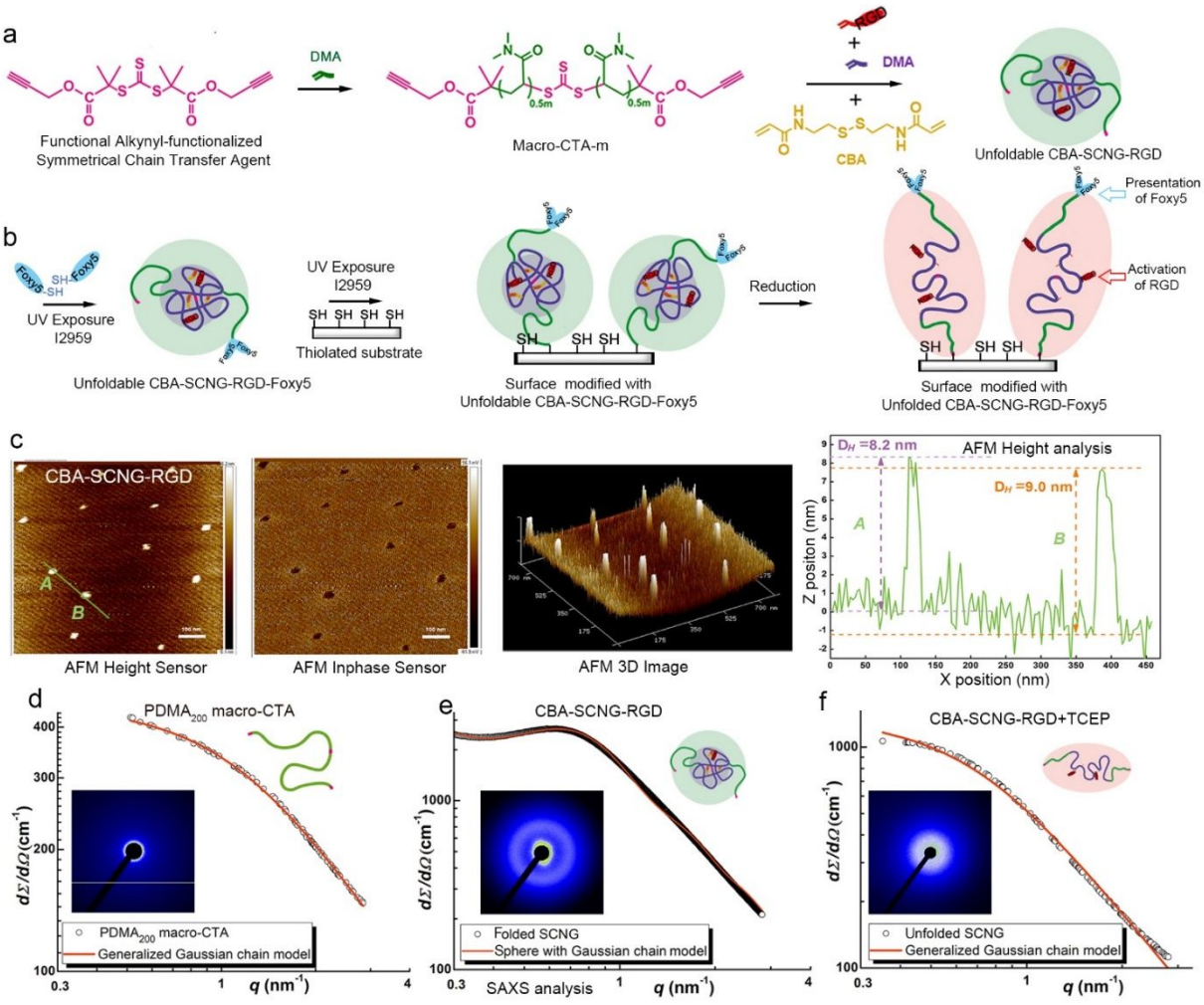

Figure 1. Preparation and characterization of unfoldable single-chain nanogels (SCNGs) with concealed RGD peptides on the substrate. (a) Synthesis route of the reduction-responsive single-chain nanogels (SCNGs) with RGD ligands hidden in the folding domain. (b) Conjugation of the Foxy5 peptide ligand to SCNGs and immobilization of the SCNGs as tunable dual-ligand co-presentation linkers onto thiolated glass substrates by thiol-yne click reaction. (c) AFM analysis of the morphology and height of the SCNGs. (d-f) SAXS data and predicted conformation of the SCNGs.

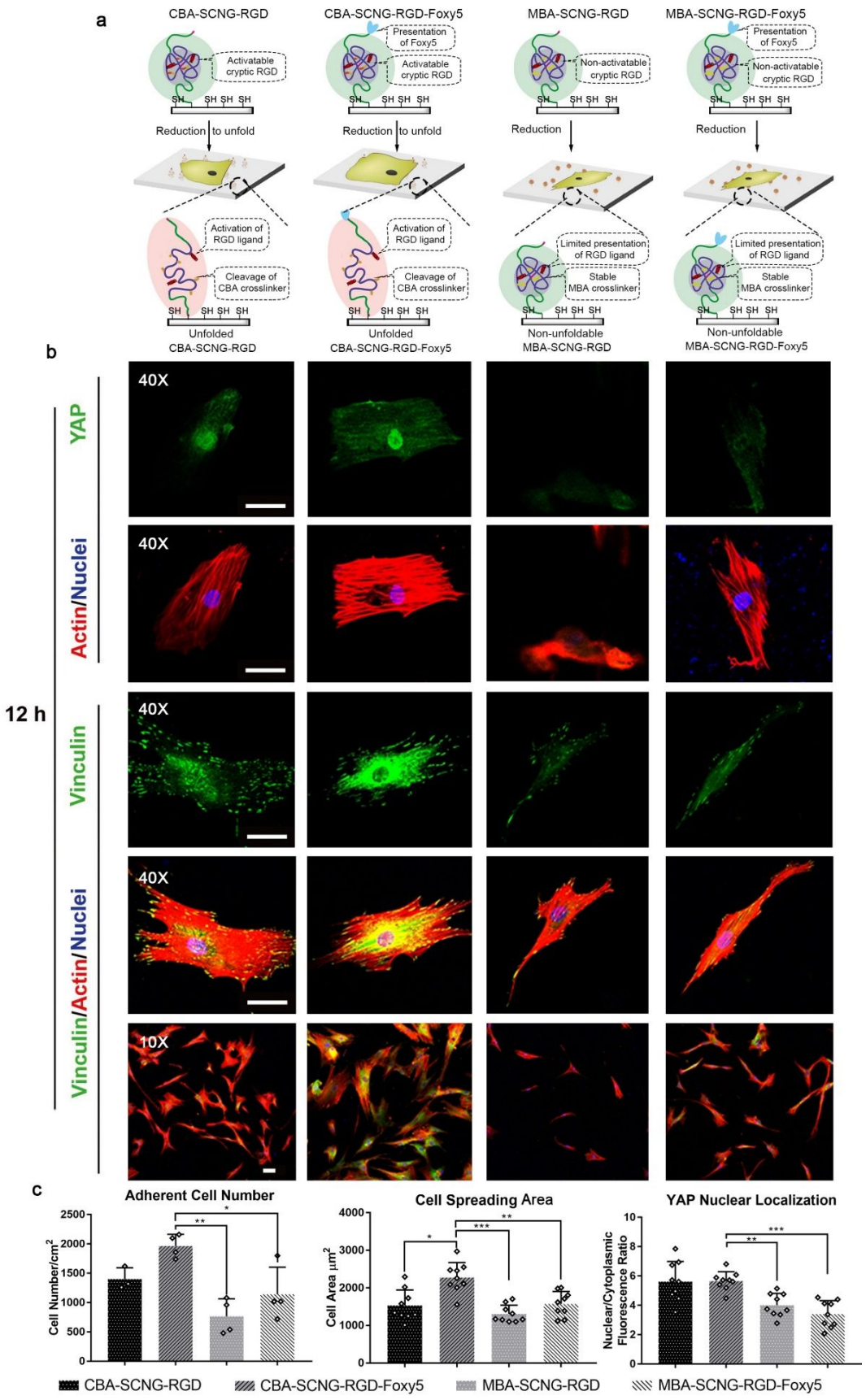
a
CBA-SCNG-RGD
CBA-SCNG-RGD-Foxy5
MBA-SCNG-RGD
MBA-SCNG-RGD-Foxy5
Activatable cryptic RGD
Presentation of Foxy5
Non-activatable cryptic RGD
Reduction to unfold
Reduction
Activation of RGD ligand
Cleavage of CBA crosslinker
Limited presentation of RGD ligand
Stable MBA crosslinker
Unfolded CBA-SCNG-RGD
Unfolded CBA-SCNG-RGD-Foxy5
Non-unfoldable MBA-SCNG-RGD
Non-unfoldable MBA-SCNG-RGD-Foxy5
b
12 h
YAP
Actin/Nuclei
Vinculin
Vinculin/Actin/Nuclei
40X
10X
c
Adherent Cell Number
Cell Number/cm2
Cell Spreading Area
Cell Area μm2
YAP Nuclear Localization
Nuclear/Cytoplasmic Fluorescence Ratio
CBA-SCNG-RGD
CBA-SCNG-RGD-Foxy5
MBA-SCNG-RGD
MBA-SCNG-RGD-Foxy5

Figure 2. Manipulation of stem cell adhesion and mechanotransduction signaling by using single-chain nanogels (SCNGs) as the stimuli-responsive macromolecular regulator of ligand presentation. (a) Cartoon illustration of surfaces with CBA-SCNGs and MBA-SCNGs for cell studies. (b) Immunofluorescence staining against YAP, vinculin, F-actin and nuclei, and (c) quantification of the adherent cell number, cell spreading area, and nuclear localization of YAP. The scale bar is 30 μm. The quantification of cell adherence was obtained from the pooled results from four independent experiments. The quantification of cell spreading area, and YAP nuclear localization was analyzed from 9 randomly-selected regions of interest (more than 7 cells in each region) from 3 independent experiments. Data are means ± SD. *P<0.05, **P<0.01, ***P<0.001 (ANOVA).

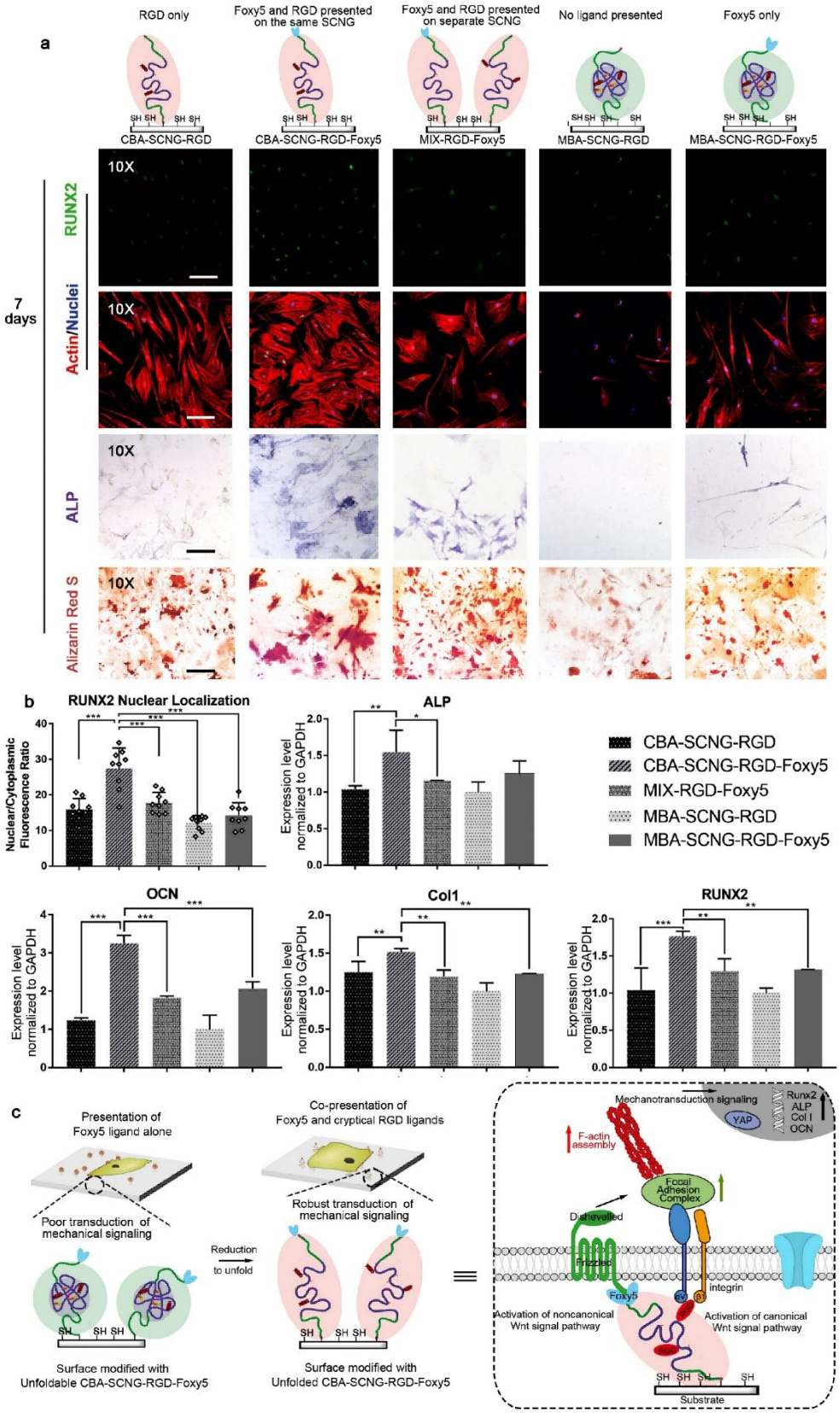
a
RGD only
Foxy5 and RGD presented on the same SCNG
Foxy5 and RGD presented on separate SCNG
No ligand presented
Foxy5 only
CBA-SCNG-RGD
CBA-SCNG-RGD-Foxy5
MIX-RGD-Foxy5
MBA-SCNG-RGD
MBA-SCNG-RGD-Foxy5
7 days
RUNX2
Actin/Nuclei
ALP
Alizarin Red S
10X
b
RUNX2 Nuclear Localization
Nuclear/Cytoplasmic Fluorescence Ratio
ALP
Expression level normalized to GAPDH
OCN
Col1
RUNX2
CBA-SCNG-RGD
CBA-SCNG-RGD-Foxy5
MIX-RGD-Foxy5
MBA-SCNG-RGD
MBA-SCNG-RGD-Foxy5
c
Presentation of Foxy5 ligand alone
Poor transduction of mechanical signaling
Surface modified with Unfoldable CBA-SCNG-RGD-Foxy5
Reduction to unfold
Co-presentation of Foxy5 and cryptical RGD ligands
Robust transduction of mechanical signaling
Surface modified with Unfolded CBA-SCNG-RGD-Foxy5
Mechanotransduction signaling
YAP
Runx2
ALP
Col I
OCN
F-actin assembly
Focal Adhesion Complex
Dishevelled
Frizzled
integrin
Foxy5
Activation of noncanonical Wnt signal pathway
Activation of canonical Wnt signal pathway
Substrate

Figure 3. Co-presentation of dual ligands on the same SCNG but not separate SCNGs synergistically enhances stem cell differentiation. (a) Images of immunofluorescence staining against RUNX2, F-actin and nuclei in different groups and staining against alkaline phosphatase (ALP) activity and calcification. The scale bar is 30 μm. (b) Quantification of the fluorescence intensity of the immunofluorescence staining of nuclear RUNX2 in each group and expression of osteogenic marker genes, including RUNX2, APL, OCN, and Col I, in hMSCs from different groups determined by PCR. The quantification of RUNX2 nuclear localization was performed in 9 randomly-selected regions of interest (more than 7 cells in each region) from 3 independent experiments. The PCR data of osteogenic marker genes were pooled for 3 independent experiments. Data are means ± SD. *P<0.05, **P<0.01, ***P<0.001 (ANOVA). (c) Mechanism of the co-presentation of dual ligands (RGD and Foxy5) on the same SCNG to induce the osteogenic differentiation of hMSCs.

ASSOCIATED CONTENT

Supporting Information.

The Supporting Information is available free of charge on the ACS Publications website. Materials, experimental methods, optical system, additional discussion, data analysis, tables and figures (PDF)

AUTHOR INFORMATION

Corresponding Author

* lbian@cuhk.edu.hk.

Author Contributions

‡These authors contributed equally. The manuscript was written through the contributions of all authors. All authors have given approval to the final version of the manuscript. The authors declare no competing financial interests.

ACKNOWLEDGMENT

This work is supported by a General Research Fund grant from the Research Grants Council of Hong Kong (project nos. 14205817, 14204618); the Health and Medical Research Fund, the Food and Health Bureau, the Government of the Hong Kong Special Administrative Region (04152836); the Chow Yuk Ho Technology Centre for Innovative Medicine, The Chinese University of Hong Kong; the CRF project (project no. C6021-14E) in MCPF of HKUST. The work was partially supported by Hong Kong Research Grants Council Theme-based Research Scheme (Ref. T13-402/17-N).

REFERENCES

1. Kang, H.; Yang, B.; Zhang, K.; Pan, Q.; Yuan, W.; Li, G.; Bian, L. Immunoregulation of Macrophages by Dynamic Ligand Presentation *via* Ligand-Cation Coordination. *Nat. Commun.***2019,** *10*, 1696.
2. Kang, H.; Zhang, K.; Jung, H. J.; Yang, B.; Chen, X.; Pan, Q.; Li, R.; Xu, X.; Li, G.; Dravid, V. P.; Bian, L. An *In Situ* Reversible Heterodimeric Nanoswitch Controlled by Metal-Ion–Ligand Coordination Regulates the Mechanosensing and Differentiation of Stem Cells. *Adv. Mater.* **2018,** *30*, 1803591.
3. Lee, T. T.; Garcia, J. R.; Paez, J. I.; Singh, A.; Phelps, E. A.; Weis, S.; Shafiq, Z.; Shekaran, A.; del Campo, A.; Garcia, A. J. Light-Triggered *In Vivo* Activation of Adhesive Peptides Regulates Cell Adhesion, Inflammation and Vascularization of Biomaterials. *Nat. Mater.* **2015,** *14*, 352-360.
4. Chaudhuri, O.; Koshy, S. T.; da Cunha, C. B.; Shin, J. W.; Verbeke, C. S.; Allison, K. H.; Mooney, D. J. Extracellular Matrix Stiffness and Composition Jointly Regulate the Induction of Malignant Phenotypes in Mammary Epithelium. *Nat. Mater.* **2014,** *13*, 970-978.

5. Cameron, A. R.; Frith, J. E.; Cooper-White, J. J. The Influence of Substrate Creep on Mesenchymal Stem Cell Behaviour and Phenotype. *Biomaterials* **2011,** *32*, 5979-5993.
6. Li, R.; Lin, S.; Zhu, M.; Deng, Y.; Chen, X.; Wei, K.; Xu, J.; Li, G.; Bian, L. Synthetic Presentation of Noncanonical Wnt5a Motif Promotes Mechanosensing-Dependent Differentiation of Stem Cells and Regeneration. *Sci. Adv.* **2019,** *5*, eaaw3896.
7. Balaban, N. Q.; Schwarz, U. S.; Riveline, D.; Goichberg, P.; Tzur, G.; Sabanay, I.; Mahalu, D.; Safran, S.; Bershadsky, A.; Addadi, L. Force and Focal Adhesion Assembly: A Close Relationship Studied Using Elastic Micropatterned Substrates. *Nat. Cell Biol.* **2001,** *3*, 466.
8. Kelsey, R. Prostate Cancer: Foxy-5 in Prostate Cancer Model. *Nat. Rev. Urol.* **2017,** *14*, 638.
9. Säfholm, A.; Leandersson, K.; Dejmek, J.; Nielsen, C. K.; Villoutreix, B. O.; Andersson, T. A Formylated Hexapeptide Ligand Mimics the Ability of Wnt-5a to Impair Migration of Human Breast Epithelial Cells. *J. Biol. Chem.* **2006,** *281*, 2740-2749.
10. Ford, C. E.; Ekström, E. J.; Howlin, J.; Andersson, T. The WNT-5a Derived Peptide, Foxy-5, Possesses Dual Properties that Impair Progression of ERα Negative Breast Cancer. *Cell Cycle* **2009,** *8*, 1838-1842.
11. Santos, A.; Bakker, A. D.; de Blieck-Hogervorst, J. M. A.; Klein-Nulend, J. WNT5A Induces Osteogenic Differentiation of Human Adipose Stem Cells *via* Rho-Associated Kinase ROCK. *Cytotherapy* **2010,** *12*, 924-932.
12. Chen, Y.-J.; Shie, M.-Y.; Hung, C.-J.; Wu, B.-C.; Liu, S.-L.; Huang, T.-H.; Kao, C.-T. Activation of Focal Adhesion Kinase Induces Extracellular Signal-Regulated Kinase-Mediated Osteogenesis in Tensile Force-Subjected Periodontal Ligament Fibroblasts but Not in Osteoblasts. *J. Bone Miner. Metab.* **2014,** *32*, 671-682.
13. Pongkitwitoon, S.; Uzer, G.; Rubin, J.; Judex, S. Cytoskeletal Configuration Modulates Mechanically Induced Changes in Mesenchymal Stem Cell Osteogenesis, Morphology, and Stiffness. *Sci. Rep.* **2016,** *6*, 34791.
14. Chaudhuri, O.; Gu, L.; Klumpers, D.; Darnell, M.; Bencherif, S. A.; Weaver, J. C.; Huebsch, N.; Lee, H.-p.; Lippens, E.; Duda, G. N. Hydrogels with Tunable Stress Relaxation Regulate Stem Cell Fate and Activity. *Nat. Mater.* **2016,** *15*, 326.
15. Matsumoto, S.; Fumoto, K.; Okamoto, T.; Kaibuchi, K.; Kikuchi, A. Binding of APC and Dishevelled Mediates Wnt5a-Regulated Focal Adhesion Dynamics in Migrating Cells. *EMBO J.* **2010,** *29*, 1192-1204.
16. Matsumoto, S.; Kikuchi, A. Regulation of Focal Adhesion Dynamics by Wnt5a Signaling. *Methods Mol. Biol.* **2012,** *839*, 215-227.
17. Kikuchi, A.; Yamamoto, H.; Sato, A.; Matsumoto, S. Wnt5a: Its Signalling, Functions and Implication in Diseases. *Acta Physiol.* **2012,** *204*, 17-33.
18. Zhu, Y.; Tian, Y.; Du, J.; Hu, Z.; Yang, L.; Liu, J.; Gu, L. Dvl2-Dependent Activation of Daam1 and RhoA Regulates Wnt5a-Induced Breast Cancer Cell Migration. *PLoS One* **2012,** *7*, e37823.
19. Kilian, K. A.; Bugarija, B.; Lahn, B. T.; Mrksich, M. Geometric Cues for Directing the Differentiation of Mesenchymal Stem Cells. *Proc. Natl. Acad. Sci. U. S. A.* **2010,** *11*, 4872-4877.
20. Witze, E. S.; Connacher, M. K.; Houel, S.; Schwartz, M. P.; Morphew, M. K.; Reid, L.; Sacks, D. B.; Anseth, K. S.; Ahn, N. G. Wnt5a Directs Polarized Calcium Gradients by Recruiting Cortical Endoplasmic Reticulum to the Cell Trailing Edge. *Dev. Cell* **2013,** *26*, 645-657.

21. Chen, X.; Li, R.; Wong, S. H. D.; Wei, K.; Cui, M.; Chen, H.; Jiang, Y.; Yang, B.; Zhao, P.; Xu, J.; Chen, H.; Yin, C.; Lin, S.; Lee, W. Y.-W.; Jing, Y.; Li, Z.; Yang, Z.; Xia, J.; Chen, G.; Li, G.; *et al.* Conformational Manipulation of Scale-Up Prepared Single-Chain Polymeric Nanogels for Multiscale Regulation of Cells. *Nat. Commun.***2019,** *10*, 2705.
22. Martino, M. M.; Tortelli, F.; Mochizuki, M.; Traub, S.; Ben-David, D.; Kuhn, G. A.; Müller, R.; Livne, E.; Eming, S. A. Hubbell, J. A. Engineering the Growth Factor Microenvironment with Fibronectin Domains to Promote Wound and Bone Tissue Healing. *Sci. Transl. Med.***2011,** *3*, 100ra89.
23. Rossier, O.; Octeau, V.; Sibarita, J.-B.; Leduc, C.; Tessier, B.; Nair, D.; Gatterdam, V.; Destaing, O.; Albiges-Rizo, C.; Tampé, R. Integrins β 1 and β 3 Exhibit Distinct Dynamic Nanoscale Organizations inside Focal Adhesions. *Nat. Cell Biol.* **2012,** *14*, 1057-1067.
24. Lowe, A. B.; Hoyle, C. E.; Bowman, C. N. Thiol-Yne Click Chemistry: A Powerful and Versatile Methodology for Materials Synthesis. *J. Mater. Chem.* **2010,** *20*, 4745-4750.
25. Fairbanks, B. D.; Scott, T. F.; Kloxin, C. J.; Anseth, K. S.; Bowman, C. N. Thiol-Yne Photopolymerizations: Novel Mechanism, Kinetics, and Step-Growth Formation of Highly Cross-Linked Networks. *Macromolecules* **2009,** *42*, 211-217.
26. Evans, E. A.; Calderwood, D. A. Forces and Bond Dynamics in Cell Adhesion. *Science* **2007,** *316*, 1148-1153.
27. Zhang, Y.; Ge, C.; Zhu, C.; Salaita, K. DNA-Based Digital Tension Probes Reveal Integrin Forces During Early Cell Adhesion. *Nat. Commun.* **2014,** *5*, 5167.
28. Gonzalez-Burgos, M.; Latorre-Sanchez, A.; Pomposo, J. A. Advances in Single Chain Technology. *Chem. Soc. Rev.* **2015,** *44*, 6122-6142.
29. Gu, Z.; Biswas, A.; Zhao, M.; Tang, Y. Tailoring Nanocarriers for Intracellular Protein Delivery. *Chem. Soc. Rev.* **2011,** *40*, 3638-3655.
30. Ye, Y.; Yu, J.; Gu, Z. Versatile Protein Nanogels Prepared by *In Situ* Polymerization. *Macromol. Chem. Phys.* **2016,** 217, 333-343.
31. Gu, Z.; Yan, M.; Hu, B.; Joo, K.-I.; Biswas, A.; Huang, Y.; Lu, Y.; Wang, P.; Tang, Y. Protein Nanocapsule Weaved with Enzymatically Degradable Polymeric Network. *Nano Lett.* **2009,** *9*, 4533-4538.
32. Sessa, R.; Yuen, D.; Wan, S.; Rosner, M.; Padmanaban, P.; Ge, S.; Smith, A.; Fletcher, R.; Baudhuin-Kessel, A.; Yamaguchi, T. P. Monocyte-Derived Wnt5a Regulates Inflammatory Lymphangiogenesis. *Cell Res.* **2016,** *26*, 262-265.
33. Linke, F.; Zaunig, S.; Nietert, M. M.; von Bonin, F.; Lutz, S.; Dullin, C.; Janovská, P.; Beissbarth, T.; Alves, F.; Klapper, W. WNT5A: A Motility-Promoting Factor in Hodgkin Lymphoma. *Oncogene* **2017,** *36*, 13-23.
34. Zhou, H.; Wu, L. The Non-Canonical Wnt Pathway Leads to Aged Dendritic Cell Differentiation. *Cell. Mol. Immunol.* **2018,** *15*, 871-872.
35. Zhou, F.; Xie, M.; Chen, D. Structure and Ultrasonic Sensitivity of the Superparticles Formed by Self-Assembly of Single Chain Janus Nanoparticles. *Macromolecules* **2014,** *47*, 365-372.
36. Zheng, Y.; Newland, B.; Tai, H.; Pandit, A.; Wang, W. Single Cyclized Molecule Structures from RAFT Homopolymerization of Multi-Vinyl Monomers. *Chem. Commun.***2012,** *48*, 3085-3087.
37. Zheng, Y.; Cao, H.; Newland, B.; Dong, Y.; Pandit, A.; Wang, W. 3D Single Cyclized Polymer Chain Structure from Controlled Polymerization of Multi-Vinyl Monomers: Beyond Flory-Stockmayer Theory. *J. Am. Chem. Soc.* **2011,** *133*, 13130-13137.

38. Gao, Y.; Newland, B.; Zhou, D.; Matyjaszewski, K.; Wang, W. Controlled Polymerization of Multivinyl Monomers: Formation of Cyclized/Knotted Single-Chain Polymer Architectures. *Angew. Chem., Int. Ed.* **2017,** *56*, 450-460.
39. Zhao, T.; Zheng, Y.; Poly, J.; Wang, W. Controlled Multi-Vinyl Monomer Homopolymerization through Vinyl Oligomer Combination as a Universal Approach to Hyperbranched Architectures. *Nat. Commun.* **2013,** *4*, 1873.
40. Pomposo, J. A.; Perez-Baena, I.; Lo Verso, F.; Moreno, A. J.; Arbe, A.; Colmenero, J. How Far Are Single-Chain Polymer Nanoparticles in Solution from the Globular State? *ACS Macro Lett.* **2014,** *3*, 767-772.
41. ter Huurne, G. M.; Gillissen, M. A. J.; Palmans, A. R. A.; Voets, I. K.; Meijer, E. W. The Coil-to-Globule Transition of Single-Chain Polymeric Nanoparticles with a Chiral Internal Secondary Structure. *Macromolecules* **2015,** *48*, 3949-3956.

For Table of Contents Only